Supporting Information

Comparing the Nature of the Active Sites in Cu-loaded SAPO-34 and SSZ-13 for the Direct Conversion of Methane to Methanol

Karoline Kvande[1,*], Dimitrios K. Pappas[1], Michael Dyballa[1], Carlo Buono[1], Matteo Signorile[2], Elisa Borfecchia[2], Kirill A. Lomachenko[3], Bjørnar Arstad[4], Silvia Bordiga[2], Gloria Berlier[2], Unni Olsbye[1], Pablo Beato[5], Stian Svelle[1]

[1] Center for Materials Science and Nanotechnology (SMN), Department of Chemistry, University of Oslo, 1033 Blindern, 0315, Oslo, Norway
[2] Department of Chemistry, NIS Center and INSTM Reference Center, University of Turin, via P. Giuria 7, 10125 Turin, Italy
[3] European Synchrotron Radiation Facility, 71 avenue des Martyrs, CS 40220, 38043 Grenoble Cedex 9, France
[4] SINTEF Industry, Department of Process Technology, Forskningsveien 1, 0373 Oslo, Norway
[5] Haldor Topsøe A/S, Haldor Topsøes Allé 1, DK-2800 Kgs. Lyngby, Denmark
* Correspondence: karoline.kvande@smn.uio.no (K.K.)

Table of Contents

1 Physico-chemical characterization

1.1 Elemental and N_2-physisorption Measurements

The results from standard characterization is reported in Table S1. The samples are denoted xCuSSZ-13 and yCuSAPO-34, where x is the Cu/Al ratio and y is the Cu/Si ratio.

Table S1. Elemental composition, such as (Al+P)/Si [Si/Al], Cu/Si [Cu/Al] and Cu content was determined with Energy Dispersive X-ray Spectroscopy (EDX). N_2-adsorption/desorption measurements recorded at -196 ℃ were used to find the specific surface area (m^2/g) and total pore volume (V_T). Thermogravimetric analysis was used to find the water content (%).

Sample	**Exchange Method (Cu-salt)**	**(Al+P)/Si [Si/Al][a]**	**Cu/Si [Cu/Al][a]**	**Cu[a] (µmol/g)**	**Water content[b] (%)**	**Specific surface area[c] (m^2/g)**	**V_T[c] (cm^3/g)**
0.50Cu SSZ-13	LIE ($CuAc_2$)	14.8	0.53	540	18	770	0.334
0.25CuSAPO-34	LIE ($CuAc_2$) (x3)[d]	14.9	0.25	249	18	616	0.294
0.08CuSAPO-34	LIE ($CuAc_2$)	14.9	0.08	87	14	690	0.306

[a]determined by EDX
[b]determined with TGA
[c]determined at $p/p_0 = 0.99$
[d]The $CuAc_2$ solution used in the first round was 0.02 M. For the second and third round, a $CuAc_2$-solution resulting in a Cu/Si ratio of 0.5 was used (0.008 M).

1.2 Scanning Electron Microscopy (SEM)

Figure S1 shows the SAPO-34 morphology at different distances.

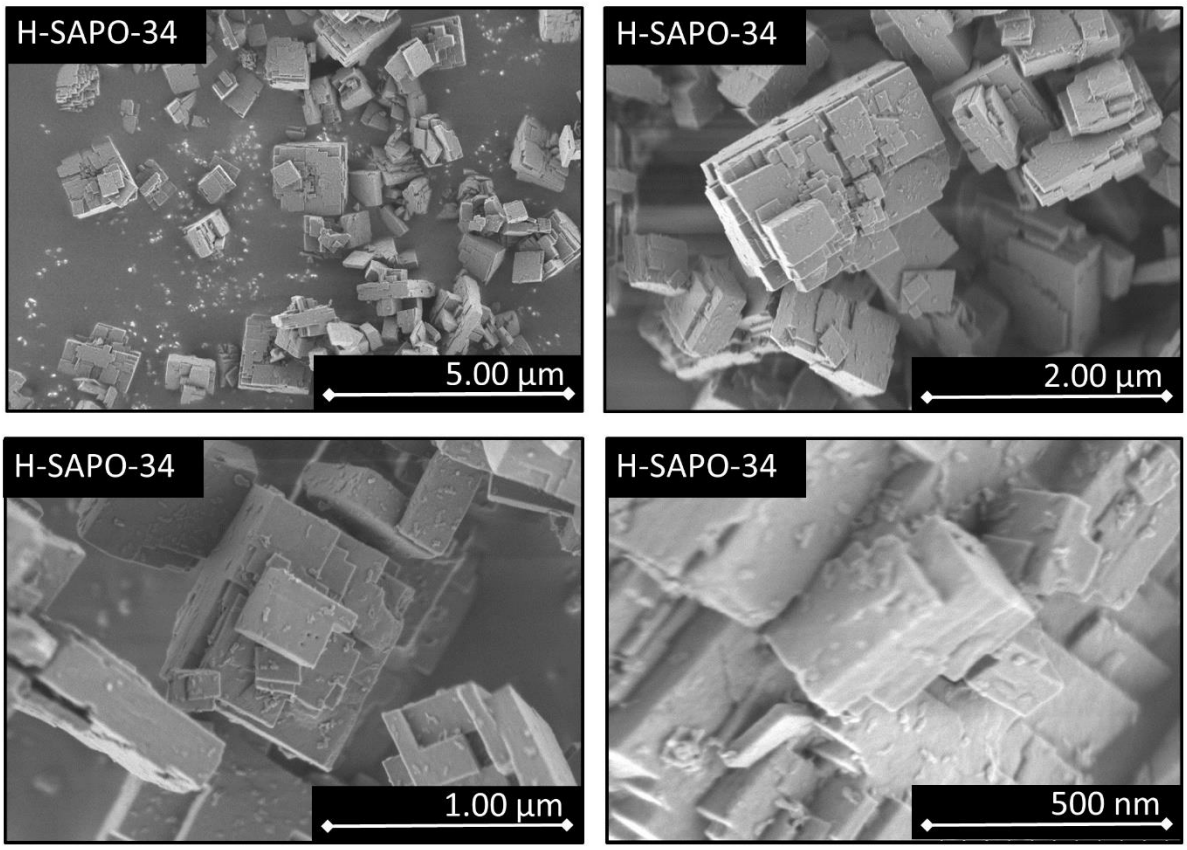

Figure S1. SEM-images of H-SAPO-34 at different distances. The crystals of the copper incorporated SAPO-34 materials were similar to the parent material, and are therefore not included.

1.3 Powder X-ray Diffraction (PXRD)

The PXRD patterns of the template containing and H-form SAPO-34 is reported in Figure S2. In Figure S3, the H-form SAPO-34 pattern is reported together with the Cu exchanged SAPO-34 samples used in this study.

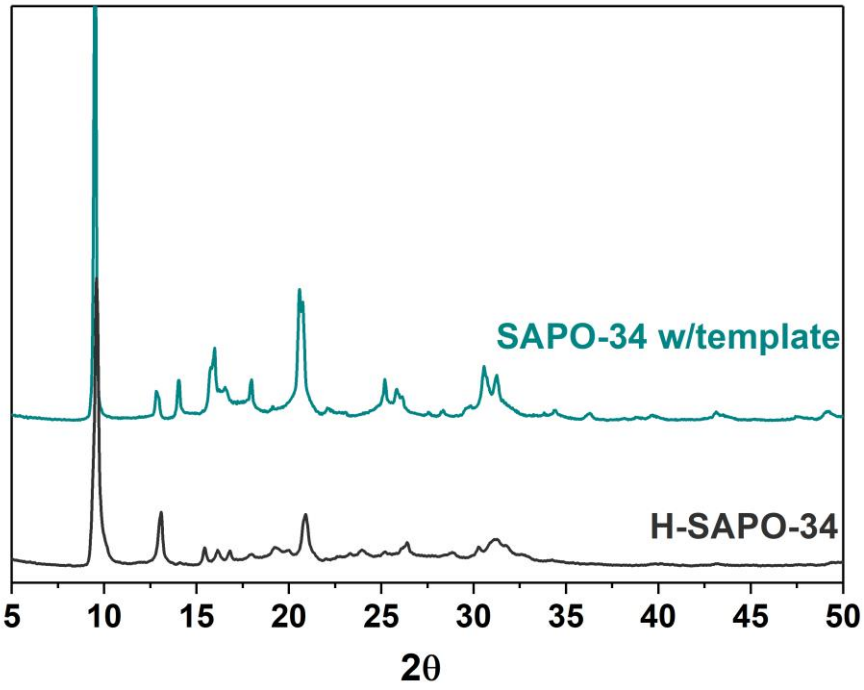

Figure S2. PXRD pattern of the template containing SAPO-34 (turquoise), and the calcined SAPO-34 (black). The patterns are vertically shifted for clarity.

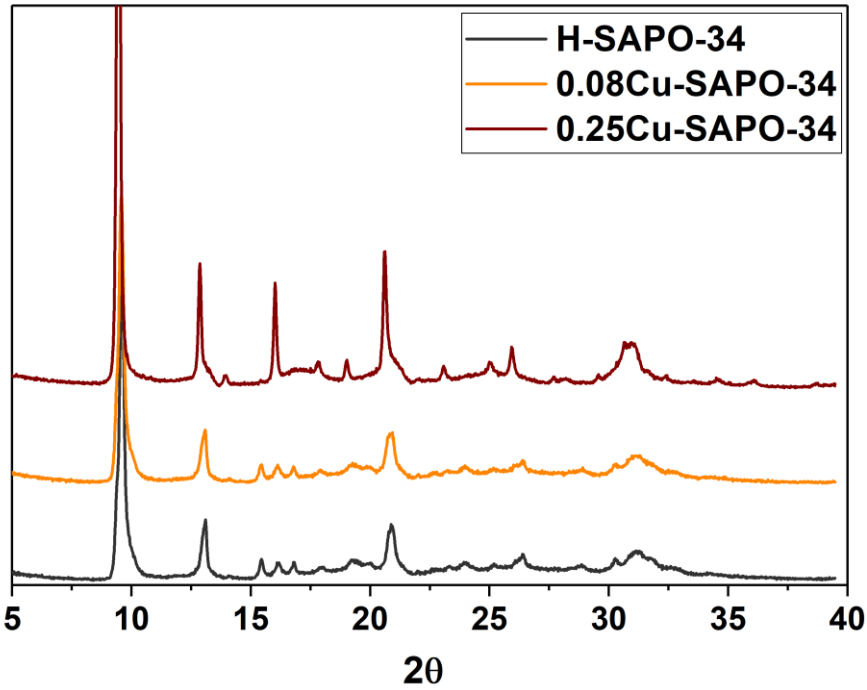

Figure S3. PXRD patterns of the calcined parent material (black) as well as the Cu-exchanged SAPO-34 materials, 0.08CuSAPO-34 (orange) and 0.25CuSAPO-34 (red). The patterns are vertically shifted for clarity.

1.4 CO_2 production from CH_4-TPR

Figure S4 shows the product detected after fully oxidation of methane over the three Cu-CHA samples tested in this study.

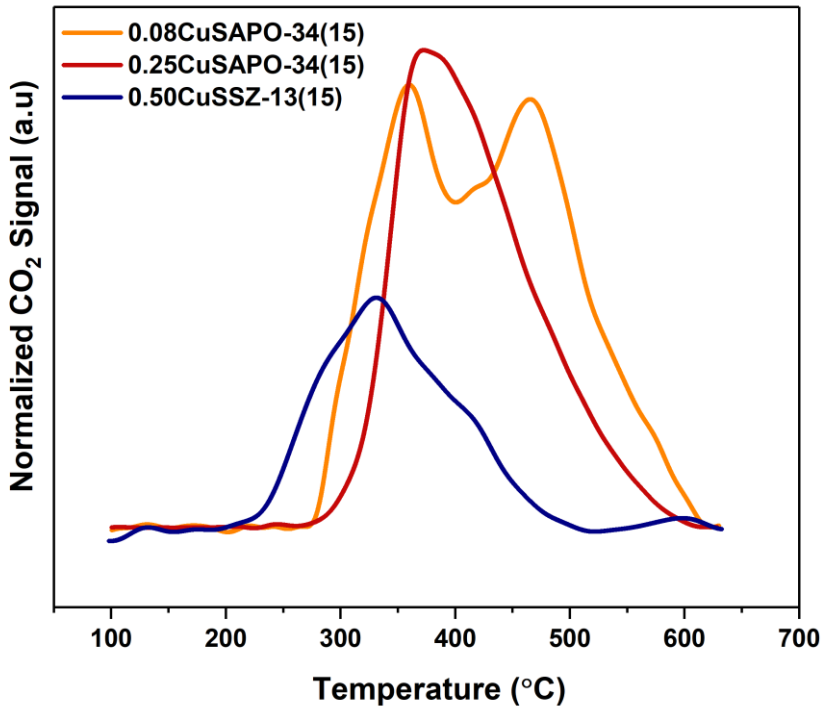

Figure S4. CO_2 production profiles from total oxidation of CH_4 over 0.50CuSSZ-13 (blue), 0.08CuSAPO-34 (orange) and 0.25CuSAPO-34 (red), measured by an online MS during flow of CH_4 while heating from 100 to 650 ℃ (ramp: 5 ℃/min). The materials were activated at 500 ℃ in O_2 for 8 h prior to the CH_4-TPR experiment. The profiles have been normalized to the sample weight.

1.5 Raman Spectroscopy

Table S2 is summary of the $Cu(II)_xO_y$ species assigned to peaks observed in the Raman spectra.

Table S2. Overview of bands correlating to $Cu(II)_xO_y$ species observed in this study, and their comparison to assignments found in literature

SAPO-34	SSZ-13	Coordination	$Cu(II)_xO_y$-species	Reference
	620	Three-fold	$[Cu\text{-}(\mu\text{-}O)\text{-}Cu]^{2+}$	Ipek et al. [1]
524	510	Three-fold	$[Cu(trans\text{-}\mu\text{-}1,2\text{-}O_2)Cu]^{2+}$	Pappas et al. [2]
587	580			
812	830			
549		Four-fold	$[Cu(\eta^2\text{-}O_2)]^{+}$	Pappas et al. [2]
1006	1100			
	1155	Three-fold	$[Cu(\eta^1\text{-}O_2)]^{+}$	Woertink et al. [3]

2 References

1. Ipek, B.; Wulfers, M. J.; Kim, H.; Göltl, F.; Hermans, I.; Smith, J. P.; Booksh, K. S.; Brown, C. M.; Lobo, R. F., Formation of $[Cu_2O_2]^{2+}$ and $[Cu_2O]^{2+}$ toward C–H Bond Activation in Cu-SSZ-13 and Cu-SSZ-39. *ACS Catal.* **2017,** *7*, 4291-4303. [10.1021/acscatal.6b03005]
2. Pappas, D. K.; Borfecchia, E.; Dyballa, M.; Pankin, I. A.; Lomachenko, K. A.; Martini, A.; Signorile, M.; Teketel, S.; Arstad, B.; Berlier, G.; Lamberti, C.; Bordiga, S.; Olsbye, U.; Lillerud, K. P.; Svelle, S.; Beato, P., Methane to Methanol: Structure-Activity Relationships for Cu-CHA. *J. Am. Chem. Soc.* **2017,** *139*, 14961-14975. [10.1021/jacs.7b06472]
3. Woertink, J. S.; Smeets, P. J.; Groothaert, M. H.; Vance, M. A.; Sels, B. F.; Schoonheydt, R. A.; Solomon, E. I., A $[Cu_2O]^{2+}$ Core in Cu-ZSM-5, the Active Site in the Oxidation of Methane to Methanol. *Proc. Natl. Acad. Sci. USA* **2009,** *106*, 18908-18913. [10.1073/pnas.0910461106]